

Antiferromagnetism and pairing in strongly correlated systems

Maciej Maška*

Department of Theoretical Physics, Silesian University, ul. Uniwersytecka 4, 40-007-PL Katowice, Poland

(Received 18 June 1996; revised manuscript received 20 September 1996)

A competition between antiferromagnetism and *s*- or *d*-wave pairing in the *t*-*J* model is analyzed beyond the mean-field level. In order to project out the states with doubly occupied sites the electronic self-energy calculated for the infinite-*U* Hubbard model is introduced in the effective Hamiltonian. Then the Green's function technique has been used to solve this approximated model. [S0163-1829(97)06805-7]

I. INTRODUCTION

It is now ten years after the unexpected discovery of high-critical-temperature superconductivity (HTSC) in the cuprates,¹ but the understanding of the phase diagram of these materials is still one of the most important issues in current physics. There is a lot of evidence that the interplay between magnetism and superconductivity is an important factor determining the mechanism of HTSC. Thus numerous works, both experimental and theoretical, have been devoted so far to understanding the "magnetic aspect" of HTSC. This paper is also dedicated to this problem: Assuming a purely electronic mechanism of HTSC, magnetic and superconducting phases are analyzed in the framework of one of the simplest models of high-*T_c* materials: the *t*-*J* model.

A common feature of the oxide superconductors is the presence of active CuO₂ layers with fourfold-coordinated copper ions and twofold-coordinated oxygen ions, separated by charge reservoir building blocks. There is considerable evidence that these layers are responsible for superconducting as well as the anomalous normal-state properties, but the charge carrier concentration is controlled by the modification of the reservoirs through the substitution or addition of oxygen.

In 1987 Anderson suggested that the one-band Hubbard Hamiltonian with a strong Coulomb repulsion can be relevant for the description of the origin of high-critical-temperature superconductivity.² This idea was based on the possibility of superconductivity arising from condensation of nearest-neighbor singlet pairs induced by Coulomb interactions, suggested in 1985 (Ref. 3) in connection with heavy-fermion systems. He proposed, as an explanation for HTSC in oxides, that single pairs (valence bonds) preexisting in a half-filled "resonating valence bond" (RVB) insulator⁴ would condensate into a superconducting state if the system were doped away from half-filling.

According to the Anderson's suggestion, the Hubbard Hamiltonian in the large-*U* limit was commonly used as a starting point. Thus numerous works have been devoted so far to clarifying the physical properties of the strong-coupling Hubbard model. Although simple in appearance, the model cannot be solved exactly except in one dimension through the Bethe ansatz.⁵ Even there, the exact solution provides only partial information about the system, and only very recently has the complete phase diagram been calculated,⁶ using a simple relation between the spectrum of

low-lying states and the correlation exponents. In more than one dimension, i.e., in the most interesting in connection with the HTSC case, the model is not exactly solvable and a variety of approximate techniques has been used to study it. The only rigorous result thought of to be applicable to higher dimensions is a theorem due to Nagaoka,⁷ the importance of which has often been exaggerated in the literature.

The Hubbard Hamiltonian is given by

$$H_{\text{Hubb}} = -t \sum_{\langle ij \rangle \sigma} (c_{i\sigma}^\dagger c_{j\sigma} + \text{H.c.}) + U \sum_i n_{i\uparrow} n_{i\downarrow}, \quad (1)$$

where $c_{i\sigma}^\dagger$ creates an electron of spin σ ($\sigma = \uparrow, \downarrow$) at site i , $n_{i\sigma} = c_{i\sigma}^\dagger c_{i\sigma}$, t is the nearest-neighbor hopping energy, and U is the on-site Coulomb repulsion. If site i is occupied by an electron of spin σ , the energy of the state with an electron of spin $-\sigma$ at site i is shifted by U relative to the state without this electron. This causes, for large enough U , the band to split into two subbands: an upper Hubbard band for electrons moving on sites which are already occupied and a lower band for electrons moving on sites which are empty. In the strong-coupling limit $U \gg t$ for $n \leq 1$ the actual hopping on occupied sites is negligible (the expectation value $\langle n_{i\sigma} n_{i-\sigma} \rangle$ is estimated to be of the order less than $e^{-(W+U)/k_B T}$, where W is the bandwidth of $U=0$ system), whereas virtual processes of this kind are possible and cause the Heisenberg spin-spin coupling. These processes in momentum space correspond to virtual electron hopping from the lower to the upper and then back to the lower subband. Thus, it is possible to carry out a canonical transformation that removes the cross-subband hopping from the Hamiltonian. Such a transformation was derived in 1977 by Chao, Spalek, and Oleś.⁸

The resulting effective Hamiltonian can be written as

$$H_{\text{eff}} = H_t^{1 \rightarrow 1} + H_t^{2 \rightarrow 2} + V + H_{\text{ex}} + H_D, \quad (2)$$

where the first and second terms describe the kinetic energy of electrons in the lower and upper subbands, respectively, V is the Coulomb interaction between two electrons on one site, and the last two terms describe interactions which originate from the cross-subband hopping: H_{ex} is the Heisenberg antiferromagnetic Hamiltonian and H_D includes hopping involving three sites. Under the condition $U \gg t$ the upper subband is empty for $n \leq 1$. Thus one can take into account only states with no doubly occupied sites. The second approxima-

tion, frequently applied to this Hamiltonian, is to neglect the interactions involving three sites. Consequently, H_{eff} taken between states with no doubly occupied sites (and upon neglecting the three-site terms) is reduced to the so-called t - J model:

$$H_{tJ} = -t \sum_{\langle ij \rangle \sigma} (1 - n_{i-\sigma}) c_{i\sigma}^\dagger c_{j\sigma} (1 - n_{j-\sigma}) + J \sum_{\langle ij \rangle} (\mathbf{S}_i \cdot \mathbf{S}_j - \frac{1}{4} n_i n_j). \quad (3)$$

In the literature one can meet some extensions to the above model. Namely, the next-nearest-neighbor hopping (the t - t' - J model), the next-nearest-neighbour exchange interaction (the t - J - J' model), or both phenomena (the t - t' - J - J' model) are taken into account. Generally, the additional interactions enhance the critical temperature⁹ and stabilize the Néel and spiral states against the phase separation.¹⁰

At half-filling each site is occupied by one electron and therefore the first term in the t - J Hamiltonian vanishes. The model becomes an antiferromagnetic Heisenberg model. This is a welcome result since the existence of antiferromagnetism has been clearly established experimentally in the new materials. Then, the most important situation corresponds to the analysis of the t - J model with doping.

Naturally, one of the crucial goals would be to understand the full phase diagram of the model. Many researchers have tried to head in this direction using various approximations. Unfortunately, these approximations are not always controlled to the extent that one would like them to be.

There are two main kinds of the approaches to the t - J model, namely, analytical and numerical. The fundamental obstacle that appears in the analytical approaches is the difficulty in handling the local constraint of strong repulsion in a satisfactory way. Therefore, apart from a few analytical results [e.g., in one dimension the t - J model is exactly solved by the Bethe-ansatz method for $J=2t$ (Ref. 11)], most work on the t - J model has been done using numerical techniques, which can handle this constraint exactly. Among others, exact diagonalization of small systems,¹² variational calculations,^{13,14} and various realizations of quantum Monte Carlo simulations¹⁵ are used to obtain the properties of this model. Unfortunately, also numerical methods meet some serious problems. As in exact diagonalization the computer time increases exponentially with the size of the system, and the method becomes of limited use, especially in more than one dimension, while the fundamental difficulty in the quantum Monte Carlo calculations is the famous sign problem, which reduces the usage of this method at low temperatures.

II. SELF-ENERGY APPROACH TO THE t - J MODEL

In the previous section it was mentioned that the single-occupancy constraint is one of the main problems which appear within analytical approaches to the t - J model. The simple renormalization of the hopping integral $t \rightarrow t' = \delta t$, proposed in the early paper of Baskaran, Zou, and Anderson,¹⁶ is not valid in the case of small δ , where the dynamics of holons becomes important.^{17,18} This approximation has been improved by Zhang *et al.*,¹⁹ who used the Gutzwiller approximation to obtain an effective Hamiltonian

with the hopping and exchange integrals replaced by the renormalized ones as follows: $t \rightarrow t' = \phi_t t$, $J \rightarrow J' = \phi_J J$, where $\phi_t = 2\delta/(1+\delta)$, $\phi_J = 4/(1+\delta)^2$.

The slave boson technique is another possible way of treating the constraint. But in the framework of this approach the single-occupancy constraint, expressed by $b_i^\dagger b_i + \sum_{\sigma} f_{i\sigma}^\dagger f_{i\sigma} = 1$, where b_i is a boson operator, representing the holon, and $f_{i\sigma}$ is a spin- $\frac{1}{2}$ neutral fermion operator, representing the spinon, is not treated rigorously either. In mean-field-type calculations the boson operators b_i are replaced by a c number $r = \langle b_i \rangle$, and thus the constraint is, in general, satisfied only on average, i.e., $\langle b_i^\dagger b_i + \sum_{\sigma} f_{i\sigma}^\dagger f_{i\sigma} \rangle = 1$. The second approximation, usually applied to the slave boson Hamiltonian, is to replace the local constraint by the global one, i.e., as an average over all lattice sites. This corresponds to taking $\lambda_i = \lambda$, independent of the lattice site.

Unfortunately, as was recently shown by Zhang *et al.*,²⁰ these approximations may lead to a significant number of doubly occupied sites, despite the infinite on-site repulsion in the original model.

The aim of this paper is to examine another approach to the constraint. This constraint originates from the strong Coulomb repulsion between two electrons of antiparallel spins at the same lattice site. The t - J Hamiltonian incorporates it by the operators $P_{i\sigma} = 1 - n_{i\sigma}$, which project out the states with doubly occupied sites. In the Hubbard model the electrons that hop on empty sites, i.e., the electrons that fulfill this constraint, are in the lower Hubbard subband, whereas the others are in the upper one. This suggests a reintroduction of the Hubbard-Coulomb term into the Hamiltonian instead of the projecting operators $P_{i\sigma}$. For large enough U this term leads to a splitting of the band into two subbands, where the lower one consists of electrons which hop on empty sites. In the case of $U = \infty$, for $n \leq 1$ the upper subband is driven out to infinity and all electrons are in the lower subband. Moreover, for $U = \infty$ the superexchange integral $J = 4t^2/U$ is equal to zero, and thus the reintroduction of the Hubbard-Coulomb term does not result in any additional spin-spin correlations.

Following this idea we propose to write the effective Hamiltonian as

$$H = -t \sum_{\langle ij \rangle \sigma} c_{i\sigma}^\dagger c_{j\sigma} + U' \sum_i n_{i\uparrow} n_{i\downarrow} + J \sum_{\langle ij \rangle} (\mathbf{S}_i \cdot \mathbf{S}_j - \frac{1}{4} n_i n_j) \quad (4)$$

$$= H'_{\text{Hubb}} + H_J, \quad (5)$$

where the prime was used to distinguish the reintroduced Coulomb energy U' from the original one. In the Hamiltonian (4) one has to put $U' = \infty$ in order to preserve the single-occupancy constraint and only in this limit is the effective Hamiltonian equal to the t - J one.

Then some approximations have to be made to make Eq. (4) soluble. As one of the approximations which is appropriate for the first two terms in Eq. (4) (H'_{Hubb}), a Green's function decoupling scheme was proposed by Hubbard with successful results in the study of the Mott-Hubbard transition²¹ (Hubbard III). The third term in the Hamiltonian (4) (H_J) is treated within the mean-field theory.

III. EFFECTIVE HAMILTONIAN

A. Kinetic part

In order to take into account the additional infinite- U' Coulomb correlations [the second term in Eq. (4)] we propose to replace electrons with hard-core quasiparticles described, in general, by the Green's function

$$G_\sigma(\mathbf{k}, \omega) = \frac{1}{\omega - \epsilon_{\mathbf{k}} - \Sigma_\sigma(\mathbf{k}, \omega)}, \quad (6)$$

where the self-energy $\Sigma_\sigma(\mathbf{k}, \omega)$ contains all irreducible scattering events. The poles

$$E_\sigma(\mathbf{k}) = \epsilon_{\mathbf{k}} + \Sigma_\sigma(\mathbf{k}, E_\sigma(\mathbf{k})) \quad (7)$$

of $G_\sigma(\mathbf{k}, \omega)$ determine the quasiparticle spectrum. This leads to the following renormalization of the one-electron Bloch energies $\epsilon_{\mathbf{k}}$:

$$\epsilon_{\mathbf{k}} \rightarrow \tilde{\epsilon}_{\mathbf{k}, \sigma}(\omega) = \epsilon_{\mathbf{k}} + \Sigma_\sigma(\mathbf{k}, \omega), \quad (8)$$

where $\Sigma_\sigma(\mathbf{k}, \omega)$ stands for the Hubbard III electronic self-energy calculated in the limit $U' \rightarrow \infty$. The same method was used in Ref. 22 with a bit more refined self-energy, which preserves the first four spectral moments, in order to study antiferromagnetism (without superconductivity) in the t - J model.

The Hubbard III approximation does admit only spatially uniform solutions, and thus one does not expect spurious antiferromagnetic phases. This is important in connection with the problem of the competition (or possibility of coexistence) between antiferromagnetism and superconductivity in HTSC materials. The self-energy $\Sigma_\sigma(\omega)$ is given by

$$\Sigma_\sigma(\omega) = \frac{U' n_{-\sigma} \omega}{\omega - U'(1 - n_{-\sigma})}, \quad (9)$$

which means that within the quasiparticle approximation any lifetime effects are neglected. Since the present analysis does not concern ferromagnetism, one may take the self-energy to be spin independent, $\Sigma_\uparrow(\omega) = \Sigma_\downarrow(\omega) = \Sigma(\omega)$. In the limit $U' \rightarrow \infty$ the self-energy (9) reduces to the form (for finite ω ; the case of finite $\omega - U'$ corresponds to the upper Hubbard subband)

$$\Sigma(\omega) = -\frac{n}{2-n}\omega, \quad (10)$$

where $n = n_\uparrow + n_\downarrow = 2n_\uparrow$.

In order to take into account an antiferromagnetic states of the Hamiltonian it is necessary to break the spin symmetry. Therefore we divide the lattice into two sublattices A and B in such a way that all neighbors of a site from sublattice A belong to sublattice B and vice versa. Then we introduce two kinds of creation (annihilation) operators $a_{\mathbf{k}, \sigma}^\dagger (a_{\mathbf{k}, \sigma})$ and $b_{\mathbf{k}, \sigma}^\dagger (b_{\mathbf{k}, \sigma})$ in the momentum space defined by

$$c_{i\sigma}^\dagger = \begin{cases} \frac{1}{\sqrt{N}} \sum_{\mathbf{k}} a_{\mathbf{k}, \sigma}^\dagger e^{-i\mathbf{k} \cdot \mathbf{R}_i} & \text{for } i \in A, \\ \frac{1}{\sqrt{N}} \sum_{\mathbf{k}} b_{\mathbf{k}, \sigma}^\dagger e^{-i\mathbf{k} \cdot \mathbf{R}_i} & \text{for } i \in B. \end{cases} \quad (11)$$

Using the above definitions the kinetic part of the effective Hamiltonian in the momentum space can be written as

$$H_t^{\text{eff}}(\omega) = \sum_{\mathbf{k}, \sigma} \tilde{\epsilon}_{\mathbf{k}}(\omega) (a_{\mathbf{k}, \sigma}^\dagger b_{\mathbf{k}, \sigma} + b_{\mathbf{k}, \sigma}^\dagger a_{\mathbf{k}, \sigma}), \quad (12)$$

where

$$\tilde{\epsilon}_{\mathbf{k}}(\omega) = \epsilon_{\mathbf{k}} - \frac{n}{2-n}\omega \quad (13)$$

and

$$\epsilon_{\mathbf{k}} = t \sum_{\langle ij \rangle} e^{i\mathbf{k} \cdot (\mathbf{R}_i - \mathbf{R}_j)}. \quad (14)$$

In the case of simple square lattice the one-particle band energies are given by

$$\epsilon_{\mathbf{k}} = -2t(\cos k_x a + \cos k_y a), \quad (15)$$

where a is the lattice constant.

B. Exchange part

In order to analyze antiferromagnetic and superconducting phases on equal footing we perform the mean-field factorization of the H_J term,

$$\begin{aligned} \mathbf{S}_i \cdot \mathbf{S}_j - \frac{1}{4} n_i n_j &\rightarrow \frac{1}{4} \langle c_{i\uparrow}^\dagger c_{i\uparrow} - c_{i\downarrow}^\dagger c_{i\downarrow} \rangle \langle c_{j\uparrow}^\dagger c_{j\uparrow} - c_{j\downarrow}^\dagger c_{j\downarrow} \rangle + \frac{1}{4} \langle c_{i\uparrow}^\dagger c_{i\uparrow} - c_{i\downarrow}^\dagger c_{i\downarrow} \rangle \langle c_{j\uparrow}^\dagger c_{j\uparrow} - c_{j\downarrow}^\dagger c_{j\downarrow} \rangle - \frac{1}{4} \langle c_{i\uparrow}^\dagger c_{i\uparrow} + c_{i\downarrow}^\dagger c_{i\downarrow} \rangle \langle c_{j\uparrow}^\dagger c_{j\uparrow} + c_{j\downarrow}^\dagger c_{j\downarrow} \rangle \\ &\quad - \frac{1}{4} \langle c_{i\uparrow}^\dagger c_{i\uparrow} + c_{i\downarrow}^\dagger c_{i\downarrow} \rangle \langle c_{j\uparrow}^\dagger c_{j\uparrow} + c_{j\downarrow}^\dagger c_{j\downarrow} \rangle - \frac{1}{2} \langle c_{i\uparrow}^\dagger c_{i\downarrow}^\dagger - c_{i\downarrow}^\dagger c_{i\uparrow}^\dagger \rangle \langle c_{j\uparrow}^\dagger c_{j\downarrow}^\dagger - c_{j\downarrow}^\dagger c_{j\uparrow}^\dagger \rangle \\ &\quad - \frac{1}{2} \langle c_{i\uparrow}^\dagger c_{i\downarrow}^\dagger - c_{i\downarrow}^\dagger c_{i\uparrow}^\dagger \rangle \langle c_{j\uparrow}^\dagger c_{j\downarrow}^\dagger - c_{j\downarrow}^\dagger c_{j\uparrow}^\dagger \rangle \\ &= \frac{1}{2} (S_i^z - \frac{1}{2} \bar{n}_i) c_{j\uparrow}^\dagger c_{j\uparrow} - \frac{1}{2} (S_i^z + \frac{1}{2} \bar{n}_i) c_{j\downarrow}^\dagger c_{j\downarrow} + \frac{1}{2} (S_j^z - \frac{1}{2} \bar{n}_j) c_{i\uparrow}^\dagger c_{i\uparrow} - \frac{1}{2} (S_j^z + \frac{1}{2} \bar{n}_j) c_{i\downarrow}^\dagger c_{i\downarrow} - \frac{1}{\sqrt{2}} \Delta_{ij}^* (c_{j\uparrow}^\dagger c_{i\downarrow} - c_{j\downarrow}^\dagger c_{i\uparrow}) \\ &\quad - \frac{1}{\sqrt{2}} \Delta_{ij} (c_{i\uparrow}^\dagger c_{j\downarrow}^\dagger - c_{i\downarrow}^\dagger c_{j\uparrow}^\dagger), \end{aligned} \quad (16)$$

where the following definitions were used

$$\bar{n}_i = \langle c_{i\uparrow}^\dagger c_{i\uparrow} + c_{i\downarrow}^\dagger c_{i\downarrow} \rangle, \quad (17)$$

$$S_i^z = \frac{1}{2} \langle c_{i\uparrow}^\dagger c_{i\uparrow} - c_{i\downarrow}^\dagger c_{i\downarrow} \rangle, \quad (18)$$

$$\Delta_{ij}^* = \frac{1}{\sqrt{2}} \langle c_{i\uparrow}^\dagger c_{j\downarrow}^\dagger - c_{i\downarrow}^\dagger c_{j\uparrow}^\dagger \rangle. \quad (19)$$

Then it is easy to show that H_J in the mean-field (MF) approximation can be written as

$$\begin{aligned} H_J^{\text{MF}} = & -J \sum_{\langle ij \rangle} \left[\bar{n}_{i\downarrow} c_{j\uparrow}^\dagger c_{j\uparrow} + \bar{n}_{i\uparrow} c_{j\downarrow}^\dagger c_{j\downarrow} \right. \\ & + \frac{1}{\sqrt{2}} \Delta_{ij} (c_{i\uparrow}^\dagger c_{j\downarrow}^\dagger - c_{i\downarrow}^\dagger c_{j\uparrow}^\dagger) \\ & \left. + \frac{1}{\sqrt{2}} \Delta_{ij}^* (c_{j\uparrow} c_{i\downarrow} - c_{j\downarrow} c_{i\uparrow}) \right], \quad (20) \end{aligned}$$

where $\bar{n}_{i\sigma}$ is defined by

$$\bar{n}_{i\sigma} = \langle c_{i\sigma}^\dagger c_{i\sigma} \rangle. \quad (21)$$

Assuming $\bar{n}_{i\sigma}$ equal for all sites of a given sublattice we introduce $n_{A\sigma}$ and $n_{B\sigma}$ by the relation

$$\bar{n}_{i\sigma} = \begin{cases} n_{A\sigma} & \text{for } i \in A, \\ n_{B\sigma} & \text{for } i \in B. \end{cases} \quad (22)$$

Then the MF Hamiltonian (20) becomes

$$\begin{aligned} H_J^{\text{MF}} = & -\frac{1}{2} z J \sum_{j \in B} \sum_{\sigma} n_{A, -\sigma} c_{j\sigma}^\dagger c_{j\sigma} \\ & -\frac{1}{2} z J \sum_{i \in A} \sum_{\sigma} n_{B, -\sigma} c_{i\sigma}^\dagger c_{i\sigma} \\ & -\frac{1}{\sqrt{2}} J \sum_{\langle ij \rangle} \sum_{\sigma} \sigma (\Delta_{ij}^* c_{j\sigma} c_{i, -\sigma} + \Delta_{ij} c_{i\sigma}^\dagger c_{j, -\sigma}^\dagger), \quad (23) \end{aligned}$$

where the coordination number z is equal to 4 for a simple square lattice. After performing the Fourier transformation one gets

$$\begin{aligned} H_J^{\text{MF}} = & -J \sum_{\mathbf{k}, \sigma} \left[\frac{z}{2} (n_{B\sigma} a_{\mathbf{k}, -\sigma}^\dagger a_{\mathbf{k}, -\sigma} + n_{A\sigma} b_{\mathbf{k}, -\sigma}^\dagger b_{\mathbf{k}, -\sigma}) \right. \\ & \left. + \frac{\sigma}{\sqrt{2}} (\Delta_{\mathbf{k}}^* b_{-\mathbf{k}, -\sigma} a_{\mathbf{k}, \sigma} + \Delta_{\mathbf{k}} a_{\mathbf{k}, \sigma}^\dagger b_{-\mathbf{k}, -\sigma}^\dagger) \right], \quad (24) \end{aligned}$$

where

$$\Delta_{\mathbf{k}} = \frac{1}{N} \sum_{\mathbf{p}\sigma} \sigma \langle b_{-\mathbf{p}, -\sigma} a_{\mathbf{p}\sigma} \rangle \gamma(\mathbf{k} - \mathbf{p}), \quad (25)$$

$$\gamma(\mathbf{k}) = 2(\cos k_x a + \cos k_y a). \quad (26)$$

IV. EQUATIONS OF MOTION FOR THE GREEN'S FUNCTIONS

Putting the terms (12) and (24) together one obtains the effective Hamiltonian

$$\begin{aligned} H_{I-J}^{\text{eff}}(\omega) = & \sum_{\mathbf{k}, \sigma} \left[\tilde{\epsilon}_{\mathbf{k}, \sigma}(\omega) (a_{\mathbf{k}, \sigma}^\dagger b_{\mathbf{k}, \sigma} + b_{\mathbf{k}, \sigma}^\dagger a_{\mathbf{k}, \sigma}) \right. \\ & - (\mu + \frac{1}{2} z J n_{B, -\sigma}) a_{\mathbf{k}, \sigma}^\dagger a_{\mathbf{k}, \sigma} \\ & - (\mu + \frac{1}{2} z J n_{A, -\sigma}) b_{\mathbf{k}, \sigma}^\dagger b_{\mathbf{k}, \sigma} \\ & \left. - \frac{1}{\sqrt{2}} \sigma J (\Delta_{\mathbf{k}} a_{\mathbf{k}, \sigma}^\dagger b_{-\mathbf{k}, -\sigma}^\dagger + \Delta_{\mathbf{k}}^* b_{-\mathbf{k}, -\sigma} a_{\mathbf{k}, \sigma}) \right], \quad (27) \end{aligned}$$

where the chemical potential μ was introduced to control the doping concentration. Then one can derive two systems of the equations of motion for the Green's functions appropriate for the evaluation of the sublattice magnetization and the RVB order parameter:

$$\mathcal{A}_\sigma(\mathbf{k}, \omega) \vec{\mathcal{G}}_\sigma(\mathbf{k}, \omega) = \vec{v}, \quad (28)$$

$$\mathcal{A}'_\sigma(\mathbf{k}, \omega) \vec{\mathcal{G}}^\dagger_\sigma(\mathbf{k}, \omega) = \vec{v}. \quad (29)$$

$\mathcal{A}_\sigma(\mathbf{k}, \omega)$ is 4×4 matrix with a block structure given by

$$\mathcal{A}_\sigma(\mathbf{k}, \omega) = \begin{pmatrix} \omega_{-\mathbf{k}} & \tilde{\Delta}_{\mathbf{k}} \\ \tilde{\Delta}_{\mathbf{k}}^\dagger & \omega_{\mathbf{k}} \end{pmatrix}, \quad (30)$$

where

$$\omega_{\mathbf{k}}^\pm = \begin{pmatrix} \omega \pm \mu \pm \frac{1}{2} z J n_{A, \mp \sigma} & \mp \tilde{\epsilon}_{\mathbf{k}, \pm \sigma}(\omega) \\ \mp \tilde{\epsilon}_{\mathbf{k}, \pm \sigma}(\omega) & \omega \pm \mu \pm \frac{1}{2} z J n_{B, \mp \sigma} \end{pmatrix}, \quad (31)$$

$$\tilde{\Delta}_{\mathbf{k}} = \begin{pmatrix} 0 & \frac{1}{\sqrt{2}} \sigma J \Delta_{-\mathbf{k}} \\ \frac{1}{\sqrt{2}} \sigma J \Delta_{\mathbf{k}} & 0 \end{pmatrix}, \quad (32)$$

$$\vec{\mathcal{G}}_\sigma(\mathbf{k}, \omega) = \begin{pmatrix} \mathcal{K}_\sigma(\mathbf{k}, \omega) \\ \mathcal{L}_\sigma(\mathbf{k}, \omega) \\ \mathcal{M}_\sigma(\mathbf{k}, \omega) \\ \mathcal{N}_\sigma(\mathbf{k}, \omega) \end{pmatrix}, \quad \vec{\mathcal{G}}^\dagger_\sigma(\mathbf{k}, \omega) = \begin{pmatrix} \mathcal{P}_\sigma(\mathbf{k}, \omega) \\ \mathcal{R}_\sigma(\mathbf{k}, \omega) \\ \mathcal{S}_\sigma(\mathbf{k}, \omega) \\ \mathcal{T}_\sigma(\mathbf{k}, \omega) \end{pmatrix}, \quad \text{and } \vec{v} = \begin{pmatrix} 0 \\ 0 \\ 0 \\ 1 \end{pmatrix}. \quad (33)$$

$\mathcal{A}'_{\sigma}(\mathbf{k}, \omega)$ can be obtained replacing in $\mathcal{A}_{\sigma}(\mathbf{k}, \omega)$ the sublattice index A by B , $\Delta_{\mathbf{k}}(\Delta_{\mathbf{k}}^*)$ by $\Delta_{-\mathbf{k}}(\Delta_{-\mathbf{k}}^*)$, and vice versa. The following symbols for the Green's functions were introduced in the above equations:

$$\begin{aligned}\mathcal{K}_{\sigma}(\mathbf{k}, \omega) &= \langle\langle a_{\mathbf{k},\sigma} | b_{-\mathbf{k},-\sigma} \rangle\rangle_{\omega}, & \mathcal{L}_{\sigma}(\mathbf{k}, \omega) &= \langle\langle a_{\mathbf{k},\sigma} | a_{-\mathbf{k},-\sigma} \rangle\rangle_{\omega}, \\ \mathcal{M}_{\sigma}(\mathbf{k}, \omega) &= \langle\langle a_{\mathbf{k},\sigma} | b_{\mathbf{k},\sigma}^{\dagger} \rangle\rangle_{\omega}, & \mathcal{N}_{\sigma}(\mathbf{k}, \omega) &= \langle\langle a_{\mathbf{k},\sigma} | a_{\mathbf{k},\sigma}^{\dagger} \rangle\rangle_{\omega},\end{aligned}\quad (34)$$

and

$$\begin{aligned}\mathcal{P}_{\sigma}(\mathbf{k}, \omega) &= \langle\langle b_{\mathbf{k},\sigma} | b_{-\mathbf{k},-\sigma} \rangle\rangle_{\omega}, & \mathcal{R}_{\sigma}(\mathbf{k}, \omega) &= \langle\langle b_{\mathbf{k},\sigma} | a_{-\mathbf{k},-\sigma} \rangle\rangle_{\omega}, \\ \mathcal{S}_{\sigma}(\mathbf{k}, \omega) &= \langle\langle b_{\mathbf{k},\sigma} | b_{\mathbf{k},\sigma}^{\dagger} \rangle\rangle_{\omega}, & \mathcal{T}_{\sigma}(\mathbf{k}, \omega) &= \langle\langle b_{\mathbf{k},\sigma} | a_{\mathbf{k},\sigma}^{\dagger} \rangle\rangle_{\omega}.\end{aligned}\quad (35)$$

The Green's functions $\mathcal{K}_{\sigma}(\mathbf{k}, \omega)$, $\mathcal{N}_{\sigma}(\mathbf{k}, \omega)$, $\mathcal{P}_{\sigma}(\mathbf{k}, \omega)$, and $\mathcal{T}_{\sigma}(\mathbf{k}, \omega)$ are needed, in general, to calculate the sublattice magnetization and the RVB order parameter in a self-consistent way. However, if one allows only antiferromagnetic and nonmagnetic phases, the symmetry $n_{A\sigma} = n_{B,-\sigma}$ can be used, and then the Green's functions $\mathcal{K}_{\sigma}(\mathbf{k}, \omega)$ and $\mathcal{N}_{\sigma}(\mathbf{k}, \omega)$ are sufficient. These functions can be obtained by solving Eqs. (28). The explicit form of $\mathcal{K}_{\sigma}(\mathbf{k}, \omega)$ and $\mathcal{N}_{\sigma}(\mathbf{k}, \omega)$ is given in the Appendix.

Applying the spectral theorem one finds for the needed expectation values

$$\langle b_{-\mathbf{k},-\sigma} a_{\mathbf{k},\sigma} \rangle = -\frac{1}{\pi} \int_{-\infty}^{\infty} f(\omega) \text{Im} \mathcal{K}_{\sigma}(\mathbf{k}, \omega + i\varepsilon) d\omega, \quad (36)$$

$$\langle a_{\mathbf{k},\sigma}^{\dagger} a_{\mathbf{k},\sigma} \rangle = -\frac{1}{\pi} \int_{-\infty}^{\infty} f(\omega) \text{Im} \mathcal{N}_{\sigma}(\mathbf{k}, \omega + i\varepsilon) d\omega, \quad (37)$$

where $f(\omega)$ is the Fermi-Dirac distribution,

$$f(\omega) = \frac{1}{e^{\beta\omega} + 1}, \quad (38)$$

with $\beta = 1/k_B T$. The poles and the residues of $\mathcal{K}_{\sigma}(\mathbf{k}, \omega)$ and $\mathcal{N}_{\sigma}(\mathbf{k}, \omega)$ are needed to calculate the integrals in the right-hand side (rhs) of Eqs. (36) and (37). It is possible to find the analytical expressions for these quantities, but they are rather useless because of their complexity. Therefore we have used numerical procedures to find these values:

$$\mathcal{K}_{\sigma}(\mathbf{k}, \omega) = \sum_{i=1}^4 \frac{\alpha_i(\mathbf{k}, \sigma)}{\omega - \omega_i(\mathbf{k}, \sigma)}, \quad (39)$$

$$\mathcal{N}_{\sigma}(\mathbf{k}, \omega) = \sum_{i=1}^4 \frac{\beta_i(\mathbf{k}, \sigma)}{\omega - \omega_i(\mathbf{k}, \sigma)}. \quad (40)$$

Substituting Eqs. (39) and (40) into Eqs. (36) and (37) one gets the expressions for $\langle b_{-\mathbf{k},-\sigma} a_{\mathbf{k},\sigma} \rangle$ and $\langle a_{\mathbf{k},\sigma}^{\dagger} a_{\mathbf{k},\sigma} \rangle$ in the following form:

$$\langle b_{-\mathbf{k},-\sigma} a_{\mathbf{k},\sigma} \rangle = \sum_{i=1}^4 \alpha_i(\mathbf{k}, \sigma) f[\omega_i(\mathbf{k}, \sigma)], \quad (41)$$

$$\langle a_{\mathbf{k},\sigma}^{\dagger} a_{\mathbf{k},\sigma} \rangle = \sum_{i=1}^4 \beta_i(\mathbf{k}, \sigma) f[\omega_i(\mathbf{k}, \sigma)]. \quad (42)$$

Then we can write equations for the RVB order parameter $\Delta_{\mathbf{k}}$ and the mean spin-up (spin-down) occupation number per site in the sublattice A and, via the relation $n_{A\sigma} = n_{B,-\sigma}$, in the sublattice B :

$$\Delta_{\mathbf{k}} = \frac{1}{N} \sum_{\mathbf{p}, \sigma} \sigma \sum_{i=1}^4 \alpha_i(\mathbf{p}, \sigma) f[\omega_i(\mathbf{p}, \sigma)] \gamma(\mathbf{p} - \mathbf{k}), \quad (43)$$

$$n_{A,\sigma} = \frac{1}{N} \sum_{\mathbf{p}} \sum_{i=1}^4 \beta_i(\mathbf{p}, \sigma) f[\omega_i(\mathbf{p}, \sigma)]. \quad (44)$$

Since $\alpha_i(\mathbf{k}, \sigma)$, $\beta_i(\mathbf{k}, \sigma)$, and $\omega_i(\mathbf{k}, \sigma)$ depend on $\Delta_{\mathbf{k}}$ and $n_{A(B),\sigma}$, the above system of equations has to be solved self-consistently in order to obtain the phase diagram of the model Hamiltonian.

V. ANTIFERROMAGNETISM VERSUS PAIRING

The most elegant way to determine the phase diagram is to assume a general form of the \mathbf{k} dependence of $\Delta_{\mathbf{k}}$, and find all the solutions of the system of equations (28), (43) and (44). Then a comparison of the free energies corresponding to these solutions will indicate the actual one. Unfortunately, such an approach requires a computational potential that definitively exceeds our possibilities.

The simplest case, when the system is soluble, is s -wave pairing with an order parameter of the form

$$\Delta_{\mathbf{k}} = \Delta^s (\cos k_x a + \cos k_y a). \quad (45)$$

However, some calculations for the case of d -wave pairing with

$$\Delta_{\mathbf{k}} = \Delta^d (\cos k_x a - \cos k_y a) \quad (46)$$

were also carried out.

Assuming s -wave pairing $\Delta_{\mathbf{k}}$ can be expressed in terms of the Bloch energy $\epsilon_{\mathbf{k}}$:

$$\Delta_{\mathbf{k}} = -\frac{\Delta^s}{2t} \epsilon_{\mathbf{k}}. \quad (47)$$

The simplicity of the case of s -wave pairing consists in the fact that then also the quantities $\alpha_i(\mathbf{k}, \sigma)$, $\beta_i(\mathbf{k}, \sigma)$, and $\omega_i(\mathbf{k}, \sigma)$ depend on \mathbf{k} only through $\epsilon_{\mathbf{k}}$. This allows us to replace the two-dimensional summation in \mathbf{k} space with a one-dimensional integration with respect to the energy, which results in a large reduction of the required CPU time.

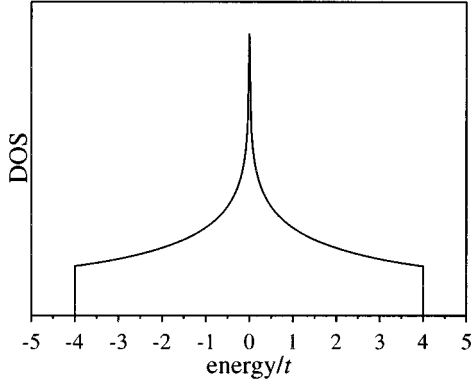


FIG. 1. Density of states for noninteracting particles on a two-dimensional square lattice with nearest-neighbor hopping.

According to Eq. (45) we can calculate Δ^s , the amplitude of s -wave pairing, as

$$\Delta^s = \frac{1}{2} \Delta_{\mathbf{k}=0} = -\frac{1}{2Nt} \sum_{\mathbf{p}, \sigma} \sigma \sum_{i=1}^4 \alpha_i(\epsilon_{\mathbf{p}}, \sigma) f[\omega_i(\epsilon_{\mathbf{p}}, \sigma)] \epsilon_{\mathbf{p}}, \quad (48)$$

where we have stressed the momentum dependence only through $\epsilon_{\mathbf{k}}$. The above equation can be rewritten using the features of the Dirac distribution δ :

$$\Delta^s = -\frac{1}{2t} \sum_{\sigma} \sigma \int_{-\infty}^{\infty} \sum_{i=1}^4 \alpha_i(\epsilon, \sigma) f[\omega_i(\epsilon, \sigma)] \epsilon \varrho(\epsilon) d\epsilon, \quad (49)$$

where $\varrho(\epsilon)$ is the density of states for noninteracting electrons defined by

$$\varrho(\epsilon) = \frac{1}{N} \sum_{\mathbf{k}} \delta(\epsilon - \epsilon_{\mathbf{k}}), \quad (50)$$

which is shown in Fig. 1.

Using the density of states $\varrho(\epsilon)$, Eq. (44), can be rewritten in an integral form

$$n_{A, \sigma} = \int_{-\infty}^{\infty} \sum_{i=1}^4 \beta_i(\epsilon, \sigma) f[\omega_i(\epsilon, \sigma)] \varrho(\epsilon) d\epsilon. \quad (51)$$

Unfortunately, for d -wave pairing the symmetry of the RVB order parameter does not allow us to do the same transformations and we have to solve the system of Eqs. (43) and (44). The amplitude of d -wave pairing Δ^d can be calculated as

$$\Delta^d = \Delta_{\mathbf{k}=(\pi/a, 0)}, \quad (52)$$

where $\Delta_{\mathbf{k}}$ is given by Eq. (46). The system of equations for $n_{A, \sigma}$ and Δ^d can be rewritten in integral form as follows:

$$\Delta^d = \int \int \sum_{\sigma} \sigma \sum_{i=1}^4 \alpha_i(k_x, k_y, \sigma) f[\omega_i(k_x, k_y, \sigma)] \gamma \times \left(k_x - \frac{\pi}{a}, 0 \right) dk_x dk_y, \quad (53)$$

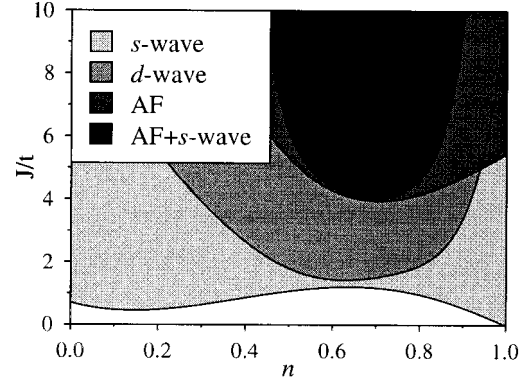


FIG. 2. Regions in the J/t - n plane where there exist antiferromagnetic, s -wave, d -wave, and antiferromagnetism + s -wave solutions.

$$n_{A, \sigma} = \int \int \sum_{\sigma} \sigma \sum_{i=1}^4 \beta_i(k_x, k_y, \sigma) f[\omega_i(k_x, k_y, \sigma)] dk_x dk_y. \quad (54)$$

A. Ground-state properties

In zero temperature the Fermi-Dirac distribution is described by the step function $\Theta(x)$. Then the ground state is determined by the following system of equations:

$$\Delta^s = -\frac{1}{2t} \int_{-\infty}^{\infty} \sum_{i=1}^4 \{ \alpha_i(\epsilon, \uparrow) \Theta[\omega_i(\epsilon, \uparrow)] - \alpha_i(\epsilon, \downarrow) \Theta[\omega_i(\epsilon, \downarrow)] \} \epsilon \varrho(\epsilon) d\epsilon, \quad (55)$$

$$n_{A, \uparrow} = \int_{-\infty}^{\infty} \sum_{i=1}^4 \beta_i(\epsilon, \uparrow) \Theta[\omega_i(\epsilon, \uparrow)] \varrho(\epsilon) d\epsilon, \quad (56)$$

$$n_{A, \downarrow} = \int_{-\infty}^{\infty} \sum_{i=1}^4 \beta_i(\epsilon, \downarrow) \Theta[\omega_i(\epsilon, \downarrow)] \varrho(\epsilon) d\epsilon, \quad (57)$$

which has been solved numerically for μ , Δ^s , and $S \equiv \frac{1}{2}(n_{A, \uparrow} - n_{A, \downarrow})$.

As the case of d -wave pairing has been treated separately because of its numerical complexity, states with mixed s - and d -wave pairing are not allowed.

For all values of the ratio J/t and $n \equiv (n_{A, \uparrow} + n_{A, \downarrow})$ there exist nonmagnetic ($S=0$) solutions without RVB ordering ($\Delta^s = \Delta^d = 0$). The regions where there exist solutions of other types [antiferromagnetism (AF), s -wave, d -wave, AF + s -wave] are presented in Fig. 2.

For $J \leq t$, s -wave pairing is allowed for a rather low hole concentration (of the order of a few percent), which agrees with results of mean-field-type as well as cluster calculations. However, this region is uninteresting for investigation of the competition or possible coexistence of antiferromagnetism and superconductivity. One can see that antiferromagnetic solutions exist only for a large (in comparison with, e.g., mean-field calculations) J . Also, the solutions with d -wave pairing appear only in the large- J region. These results originate from a different treatment of the single-occupancy constraint. In all mean-field-type approaches the

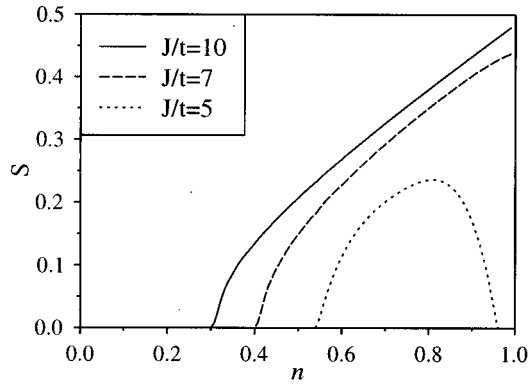


FIG. 3. AF order parameter S as a function of the occupation number n .

bandwidth is renormalized and tends to zero when the system becomes undoped. Thus the value of the exchange parameter J relative to the bandwidth W is proportional to δ^{-1} , $J/W \propto J/\delta t$, and tends to infinity when the system goes to the half-filling limit. This is not the case of the present approach. Equation (8), which contains the main idea of this approach, does not lead to such a band narrowing. The band is wider than within the mean-field-like approximations and smaller values of the hopping integral t are enough to destroy the antiferromagnetic ordering. Thus, there is no simple correspondence between the original t - J model (3) parameters and the parameters of the Hamiltonian (27), especially for small doping, when the influence of the hard-core potential U' [Eq. (4)] is dominant. (The validity of the present approximation in this region is a separate problem and will be discussed later.) Therefore we prefer to consider J/t as a parameter of an independent Hamiltonian, not connected via equation $J/t = 4t/U$ with the Hubbard U and t . Under such an assumption one can study the effective Hamiltonian for an arbitrary value of J/t , not only in the limit of small J/t , when the t - J model is equivalent to the Hubbard one.

Figure 3 presents the dependence of the antiferromagnetic order parameter S on the occupancy number n for various values of the ratio J/t , whereas the RVB order parameters Δ^s and Δ^d in the cases of “pure” s - and d -wave RVB states are presented in Figs. 4 and 5, respectively.

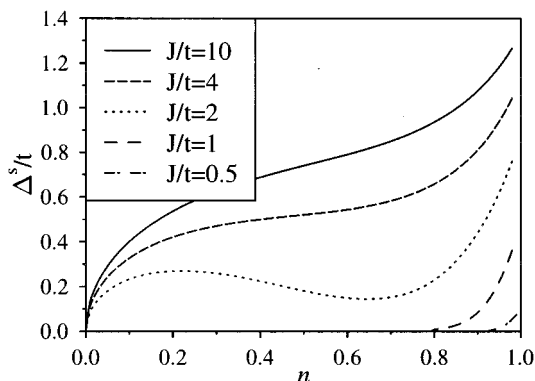


FIG. 4. Extended s -wave RVB order parameter as a function of the occupation number n .

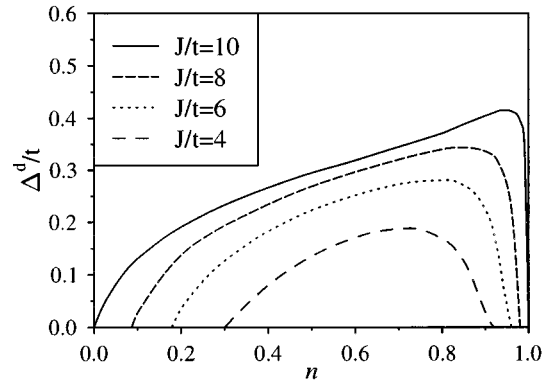


FIG. 5. d -wave RVB order parameter as a function of the occupation number n .

There exist also solutions with coexisting AF and s -wave phases, represented by the solid lines in Fig. 6.

In the regions in the J/t - n plane, where several solutions are found, the corresponding energies have to be compared in order to determine the actual ground state. These energies can be obtained integrating the chemical potential with respect to the particle number

$$E = \int_0^n \mu(n') dn'. \quad (58)$$

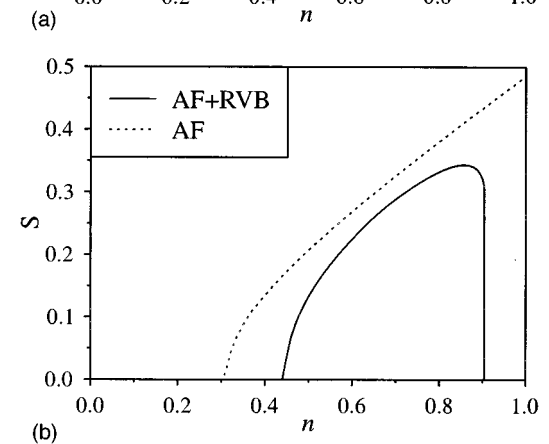
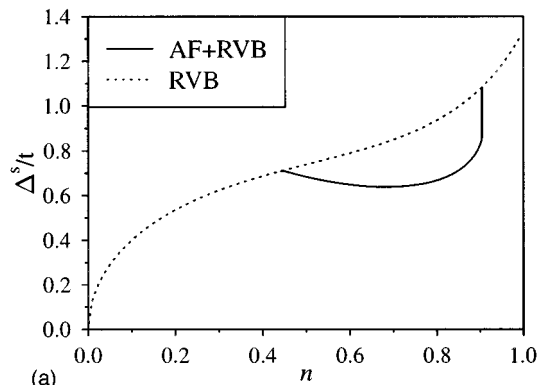


FIG. 6. Extended s -wave RVB (a) and AF (b) order parameters in the case of the coexistence of s -wave pairing and antiferromagnetism for $J/t = 10$. The dotted lines show the values of Δ^s and S for “pure” RVB and AF solutions.

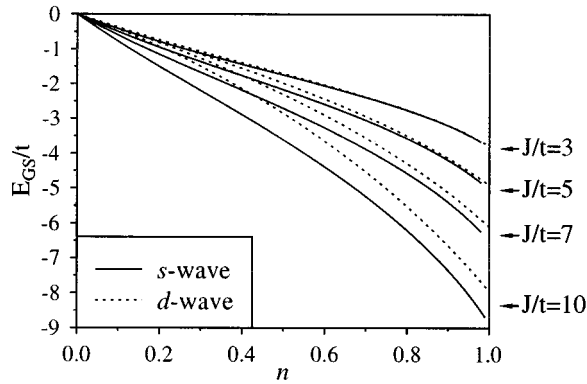


FIG. 7. Comparison of ground-state energies between s - and d -wave phases.

The comparisons between s - and d -wave and between AF and s -wave ground-state energies are given in Figs. 7 and 8, respectively.

Figure 9 shows the regions of stability of different solutions. We found that in the small- J limit the model exhibits s -wave pairing only for n close to 1, whereas for $J > t$, s -wave pairing is allowed for arbitrary values of n . Above $J/t \sim 5$ for $n > 0.7$ the RVB state becomes unstable towards a phase transition to the AF ordering. Note that comparison of the energies does not allow the coexistence of antiferromagnetism and s -wave superconductivity.

Also, we have not found regions where the d -wave solution minimizes the energy.

Of course, the phase diagram is far from complete. At least the RVB phases with an order parameter of mixed s and d types, which can be studied on an equal footing with the pure s - and d -wave pairing within the present approach, should be marked.

B. Finite-temperature results

The results from the previous section have been extended to the case of finite temperature, by solving the system of Eqs. (49) and (51) with the Fermi function instead of the step function. The absence of regions with stable d -wave zero-temperature solutions gives no motivation for finite-temperature calculations in the d -wave phase. Thus, we have

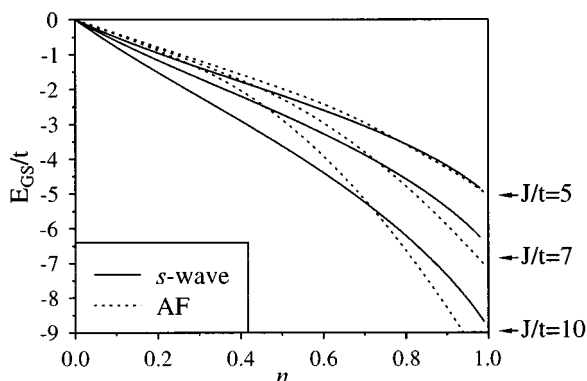


FIG. 8. Comparison of ground-state energies between s -wave and AF phases.

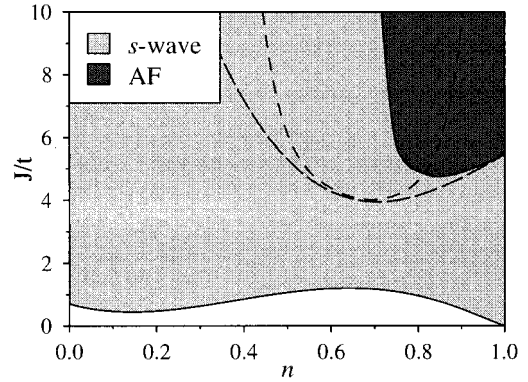


FIG. 9. Zero-temperature phase diagram of the t - J model in the present approximation. The dashed lines show the bounds of the regions where different solutions exist (the same as in Fig. 2).

calculated only the Néel temperature T_N and the temperature of the s -wave RVB transition T_{RVB} . The results are presented in Figs. 10 and 11. Figure 12 shows the finite temperature phase diagram for $J/t = 7$.

Both critical temperatures T_{RVB} and T_N increase monotonically with occupation number n (excluding the case of small J/t , when T_{RVB} has a local minimum for $n = 0.1-0.2$), reaching the highest values for $n = 1$. For a low band filling T_{RVB} is higher than T_N , whereas for high band filling T_{RVB} is lower than T_N . The situation resembles the diagram of stability of the zero-temperature RVB and antiferromagnetic phases (Fig. 9). For n close to 1 the increase of the critical temperatures is very rapid. Such a tendency results from the approximation applied within the present approach, which is invalid in the region where effects of localization dominate.

Note that T_{RVB} may be not equivalent to the superconducting critical temperature T_c , at least in some regions in the n - J/t plane. Since the exact scenario of superconductivity within the RVB approach is still an open question, one should not directly compare this critical temperature with the actually observed superconducting transition temperature. For instance, the RVB ordering can be present in undoped materials, whereas superconductivity has to vanish because of the lack of the charge carriers. Thus, T_{RVB} different from zero for $n = 1$ is not an unphysical result and does not ex-

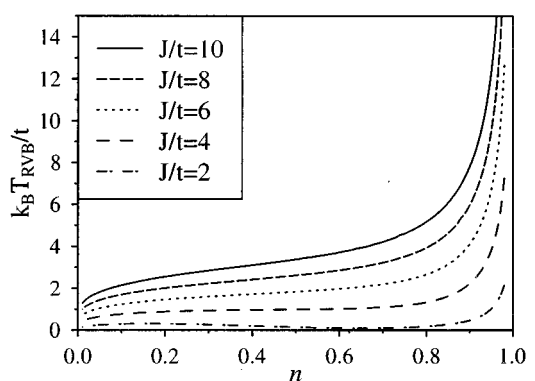


FIG. 10. Extended s -wave RVB transition temperature T_{RVB} as a function of the occupation number n .

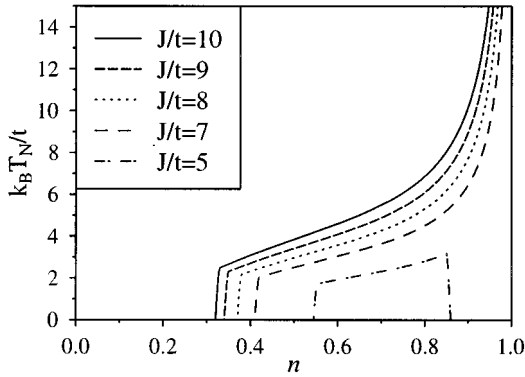


FIG. 11. Néel temperature as a function of the occupation number n .

clude T_c being equal to zero. See, for example, Refs. 17 and 18 and where the onset temperatures of the RVB (T_{RVB}), coherent motion of holons (T_D), and the Bose condensation of holons (T_B) are taken into account. The critical temperature of superconductivity is then chosen as the lowest of T_{RVB} , T_D , and T_B , and is equal to zero for $n=1$ despite finite T_{RVB} .

VI. PHASE SEPARATION

So far the stability of different phases was analyzed at a fixed concentration of holes. However, phases which are absolutely stable when the concentration of holes is fixed could be unstable if one allows density fluctuations. Such a situation was considered by Visher.²³ He proposed that the Hubbard model in the small-doping regime phase separates into a hole-rich phase and a hole-poor phase. This scenario has been recently revived as a generic feature of the t - J model close to half-filling.²⁴ This phase-separation state means that all of the doped holes exist in one phase, while the other phase is the undoped pure antiferromagnetic Heisenberg spin system. In high- T_c superconductors the macroscopic phase-separation has been observed in oxygen-doped La_2CuO_4 and in photodoped materials.^{25–28} In Ref. 24 a distinction was made between two mechanisms leading to phase separation. When $J \gg t$ holes are segregated in order to spare antiferromagnetic bonds breaking. On the other hand, in the small- J regime ($J \ll t$), the holes polarize ferromagnetically the spin background in order to minimize their own kinetic energy and are then collected in large ferromagnetic bubbles. Since in the present approximation antiferromagnetism appears for large J , one can expect that the first of the mechanisms will produce phase separation. Such a phase separation appears if the gain in exchange energy by adding an electron to the antiferromagnetic phase outweighs the cost in kinetic energy. Figures 7 and 8 show the ground-state energies as a function of occupation number n in the antiferromagnetic and RVB cases calculated for spatially uniform phases. Unfortunately, since our approximation is not valid in the case of $n=1$, e.g., in the Heisenberg (hole-free) phase, it is not possible to determine the bounds of the regions of a stable phase-separation state from this figure. However, it is apparent that the second derivative of the ground-state energy $E_0 = E_0(n)$ in both the phases (AF and RVB) is negative for

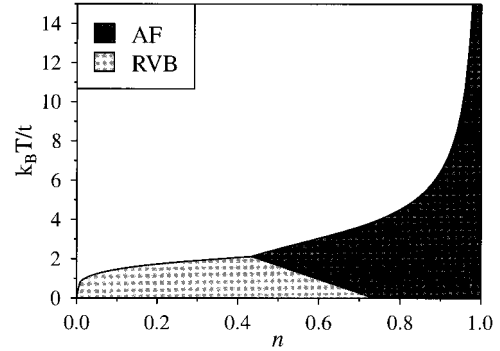


FIG. 12. Finite-temperature phase diagram for $J/t=7$.

n close to 1. This guarantees the presence of the phase separation. An argument going back to Maxwell and Gibbs^{29,30} asserts that the free energy of a system must always be a convex function of density: Otherwise, one can always construct a phase-separated state of lower and convex free energy. The regions of upward concavity increase with the increase of the value of J/t , and for large enough J/t it seems that phase separation appears for an arbitrary hole concentration.

Of course phase separation may result from the simplicity of the model. If phase separation were to lead to the formation of highly charged regions, the Coulomb force would surely prevent its occurrence, but the t - J model does not include intersite interactions. However, phase separation could then take place if negatively charged ions also separate, compensating the hole-charge imbalance.

VII. DISCUSSION

Finally it is necessary to make some comments on the validity of the proposed approach to high- T_c systems. Let us leave alone the debate on the question if the t - J model is relevant to describe the low-energy properties of CuO_2 planes.^{31–35} However, the approximation derived in this work does not claim to be valid for arbitrary values of the model parameters. It is a proposition how to approach the famous single-occupancy constraint beyond the slave particle (SP) formalism. The approximation is based on the electronic self-energy, used to renormalize the one-particle energies $\epsilon_{\mathbf{k}}$. The main difference between the proposed approximation and the SP approaches appears in the small-doping regime. In the SP approaches the density of states tends to the Dirac δ as the occupation number n goes to 1 (the bandwidth is proportional to δt , where $\delta \equiv 1 - n$), whereas in the present approximation the bandwidth remains finite for an arbitrary hole concentration. Thus, in the half-filling limit the Heisenberg model is not recovered. This is a result of the Hubbard III approximation, which does not reproduce the Curie law for the magnetic susceptibility, in the Hubbard model with infinite U for $n=1$. This is the main disadvantage of the proposed approximation, and one can expect a wrong behavior of the model in the small-doping region (unfortunately, a very interesting region). Indeed, Figs. 10 and 11 show a very strong increase of the critical temperatures T_N and T_{RVB} for $n \rightarrow 1$, whereas T_N is expected to be finite and T_{RVB} is expected to be finite or zero. It also may

lead to such strong exchange interactions needed to obtain antiferromagnetism near half-filling.

Some improvement to the Hubbard III decoupling scheme has been made by Kawabata.^{36,37} The improved Hubbard III approximation was later applied to the t - J model,^{38,39} and it can be the starting point for extending the validity of the proposed approach to the nearly half-filled case.

The self-energy approach to the single-occupancy constraint, adopted in the present work, modifies the one-particle properties of electrons, and hence could be applied only to the kinetic term of the t - J Hamiltonian. Therefore, we were not able to treat both the kinetic and exchange parts at the same level, restricting the treatment of the exchange term to the mean-field approximation. However, since the J term does not change the number of electrons at a given site, we do not expect that this approach results in the violation of the single-occupancy constraint.

ACKNOWLEDGMENTS

This work was partially supported by the Polish State Committee for Scientific Research under Grant No. 2 P03B 079 09.

APPENDIX: GREEN'S FUNCTIONS \mathcal{K} AND \mathcal{N}

Generally, the Green's functions $\mathcal{K}_\sigma(\mathbf{k}, \omega)$ and $\mathcal{N}_\sigma(\mathbf{k}, \omega)$, calculated from Eq. (28), are very complicated quantities. However, restricting magnetic solutions to an antiferromagnetism, we can use the following symmetries in order to simplify these functions:

$$n_{A,\sigma} = n_{B,-\sigma} = n_\sigma, \quad \Delta_{\mathbf{k}} = \Delta_{-\mathbf{k}}, \quad \epsilon_{\mathbf{k}} = \epsilon_{-\mathbf{k}}. \quad (\text{A1})$$

Then, $\mathcal{K}_\sigma(\mathbf{k}, \omega)$ and $\mathcal{N}_\sigma(\mathbf{k}, \omega)$ can be expressed as follows:

$$\mathcal{K}_\sigma(\mathbf{k}, \omega) = \frac{\sum_{i=0}^2 \alpha_{i,\sigma} \omega^i}{\sum_{i=0}^4 \delta_{i,\sigma} \omega^i}, \quad (\text{A2})$$

$$\mathcal{N}_\sigma(\mathbf{k}, \omega) = \frac{\sum_{i=0}^3 \beta_{i,\sigma} \omega^i}{\sum_{i=0}^4 \delta_{i,\sigma} \omega^i}, \quad (\text{A3})$$

where $\alpha_{i,\sigma}$, $\beta_{i,\sigma}$, and $\delta_{i,\sigma}$ are given by

$$\alpha_{0,\sigma} = \epsilon_{\mathbf{k}}^2 \frac{1}{\sqrt{2}} J \Delta_{\mathbf{k}} + \frac{1}{4} J^3 \Delta_{\mathbf{k}}^3 + \frac{1}{\sqrt{2}} J \Delta_{\mathbf{k}} \left(\mu + \frac{1}{2} z J n_\sigma \right)^2, \quad (\text{A4})$$

$$\alpha_{1,\sigma} = 2 \epsilon_{\mathbf{k}} \frac{1}{\sqrt{2}} J \Delta_{\mathbf{k}} \frac{n}{2-n}, \quad (\text{A5})$$

$$\alpha_{2,\sigma} = \frac{1}{\sqrt{2}} J \Delta_{\mathbf{k}} \left[\left(\frac{n}{2-n} \right)^2 - 1 \right], \quad (\text{A6})$$

$$\beta_{0,\sigma} = \frac{1}{2} J^2 \Delta_{\mathbf{k}}^2 \left(\mu + \frac{1}{2} z J n_\sigma \right) + \left(\mu + \frac{1}{2} z J n_{-\sigma} \right)^2 \times \left(\mu + \frac{1}{2} z J n_\sigma \right) - \epsilon_{\mathbf{k}}^2 \left(\mu + \frac{1}{2} z J n_{-\sigma} \right), \quad (\text{A7})$$

$$\beta_{1,\sigma} = -\epsilon_{\mathbf{k}}^2 - \frac{1}{2} J^2 \Delta_{\mathbf{k}}^2 \left(\mu + \frac{1}{2} z J n_{-\sigma} \right)^2 - 2 \epsilon_{\mathbf{k}} \left(\mu + \frac{1}{2} z J n_{-\sigma} \right) \frac{n}{2-n}, \quad (\text{A8})$$

$$\beta_{2,\sigma} = -\left(\mu + \frac{1}{2} z J n_{-\sigma} \right) - 2 \epsilon_{\mathbf{k}} \frac{n}{2-n} - \left(\mu + \frac{1}{2} z J n_{-\sigma} \right) \left(\frac{n}{2-n} \right)^2, \quad (\text{A9})$$

$$\beta_{3,\sigma} = 1 - \left(\frac{n}{2-n} \right)^2, \quad (\text{A10})$$

$$\delta_{0,\sigma} = \epsilon_{\mathbf{k}}^4 + \epsilon_{\mathbf{k}}^2 J^2 \Delta_{\mathbf{k}}^2 + \frac{1}{4} J^4 \Delta_{\mathbf{k}}^4 + \frac{1}{2} J^2 \Delta_{\mathbf{k}}^2 \left(\mu + \frac{1}{2} z J n_{-\sigma} \right)^2 - 2 \epsilon_{\mathbf{k}}^2 \left(\mu + \frac{1}{2} z J n_{-\sigma} \right) \left(\mu + \frac{1}{2} z J n_\sigma \right) + \frac{1}{2} J^2 \Delta_{\mathbf{k}}^2 \times \left(\mu + \frac{1}{2} z J n_\sigma \right)^2 + \left(\mu + \frac{1}{2} z J n_{-\sigma} \right)^2 \left(\mu + \frac{1}{2} z J n_\sigma \right)^2, \quad (\text{A11})$$

$$\delta_{1,\sigma} = 4 \epsilon_{\mathbf{k}} \frac{n}{2-n} \left[\epsilon_{\mathbf{k}}^2 + \frac{1}{2} J^2 \Delta_{\mathbf{k}}^2 - \left(\mu + \frac{1}{2} z J n_{-\sigma} \right) \left(\mu + \frac{1}{2} z J n_\sigma \right) \right] \quad (\text{A12})$$

$$\delta_{2,\sigma} = 6 \epsilon_{\mathbf{k}}^2 \left(\frac{n}{2-n} \right)^2 - 2 \epsilon_{\mathbf{k}}^2 - J^2 \Delta_{\mathbf{k}}^2 - \left(\mu + \frac{1}{2} z J n_{-\sigma} \right)^2 - \left(\mu + \frac{1}{2} z J n_\sigma \right)^2 + J^2 \Delta_{\mathbf{k}}^2 \left(\frac{n}{2-n} \right)^2 - 2 \left(\mu + \frac{1}{2} z J n_{-\sigma} \right) \times \left(\mu + \frac{1}{2} z J n_\sigma \right) \left(\frac{n}{2-n} \right)^2, \quad (\text{A13})$$

$$\delta_{3,\sigma} = 4 \epsilon_{\mathbf{k}} \frac{n}{2-n} \left[\left(\frac{n}{2-n} \right)^2 - 1 \right], \quad (\text{A14})$$

$$\delta_{4,\sigma} = \left[\left(\frac{n}{2-n} \right)^2 - 1 \right]^2. \quad (\text{A15})$$

It is possible to find analytical forms of the poles and the residua of $\mathcal{K}_\sigma(\mathbf{k}, \omega)$ and $\mathcal{N}_\sigma(\mathbf{k}, \omega)$, but the fastest way is to do it numerically, and such a method was used in the present calculations.

*Electronic address: maciek@risc3.phys.us.edu.pl

¹J. G. Bednorz and K. A. Müller, Z. Phys. B **64**, 189 (1986).

²P. W. Anderson, Science **235**, 1196 (1987).

³J. E. Hirsch, Phys. Rev. Lett. **54**, 1317 (1985).

⁴P. W. Anderson, Mater. Res. Bull. **8**, 153 (1973); P. Fazekas and P. W. Anderson, Philos. Mag. **30**, 432 (1974).

⁵E. H. Lieb and F. Y. Wu, Phys. Rev. Lett. **20**, 1445 (1968).

⁶M. Ogata and H. Shiba, Phys. Rev. B **41**, 2326 (1990); A. Parola

- and S. Sorella, Phys. Rev. Lett. **64**, 1831 (1990); H. J. Schulz, *ibid.* **64**, 2831 (1990).
- ⁷Y. Nagaoka, Phys. Rev. **147**, 392 (1966).
- ⁸K. A. Chao, J. Spátek, and A. M. Oleś, J. Phys. C **10**, L271 (1977).
- ⁹J. Zielinski, M. Matlak, and P. Entel, Phys. Lett. A **136**, 441 (1989).
- ¹⁰G. C. Psaltakis and N. Papanicolaou, Phys. Rev. B **48**, 456 (1993).
- ¹¹P. Schlottmann Phys. Rev. B **36**, 5177 (1987); P.-A. Bares, G. Blatter, and M. Ogata, *ibid.* **44**, 130 (1991).
- ¹²E. Dagotto, Int. J. Mod. Phys. B **5**, 77 (1991); J. Bonča, P. Prelovšek, and I. Sega, Phys. Rev. B **39**, 7074 (1989); E. Dagotto, R. Joynt, A. Moreo, S. Bacci, and E. Gagliano, *ibid.* **41**, 9049 (1990); C.-X. Chen and H. B. Schütler, *ibid.* **40**, 239 (1989); K. Szczepanski, R. Horsch, W. H. Stephan, and M. Ziegler, *ibid.* **41**, 2017 (1990); N. Furukawa and M. Imada, J. Phys. Soc. Jpn. **59**, 1771 (1990); E. Dagotto, Rev. Mod. Phys. **66**, 763 (1994).
- ¹³H. Yokoyama and H. Shiba, J. Phys. Soc. Jpn. **57**, 2483 (1988); C. Gros, R. Joynt, and T. M. Rice, Z. Phys. B **68**, 425 (1987); T. K. Lee and S. Feng, Phys. Rev. B **38**, 11809 (1988); R.R.P. Singh, M. Gelfand, and D. A. Huse, Phys. Rev. Lett. **61**, 2484 (1988).
- ¹⁴C. Gros, Ann. Phys. (N.Y.) **189**, 53 (1989).
- ¹⁵S. Tang and J. E. Hirsch, Phys. Rev. B **39**, 4548 (1989); S. Sorella, S. Baroni, R. Car, and M. Parinello, Europhys. Lett. **8**, 663 (1989); M. Imada, J. Phys. Soc. Jpn. **58**, 2650 (1989); I. Morgenstern, Z. Phys. B **73**, 299 (1989); **77**, 267 (1989); S. R. White, D. J. Scalapino, R. L. Sugar, and N. E. Bickers, Phys. Rev. Lett. **63**, 1523 (1989); S. R. White, D. J. Scalapino, R. L. Sugar, N. E. Bickers, and R. T. Scaletler, Phys. Rev. B **39**, 839 (1989).
- ¹⁶G. Baskaran, Z. Zou, and P. W. Anderson, Solid State Commun. **63**, 973 (1987).
- ¹⁷H. Fukuyama, Y. Hasegawa, and Y. Suzumura, Physica C **153–155**, 1630 (1988).
- ¹⁸H. Fukuyama, Int. J. Mod. Phys. B **1**, 577 (1988).
- ¹⁹F. C. Zhang, C. Gros, T. M. Rice, and H. Shiba, Supercond. Sci. Technol. **1**, 36 (1988).
- ²⁰L. Zhang, J. K. Jain, and V. J. Emery, Phys. Rev. B **47**, 3368 (1993).
- ²¹J. Hubbard, Proc. R. Soc. London A **276**, 283 (1963); **281**, 401 (1964).
- ²²M. Maška, Phys. Rev. B **48**, 1160 (1993).
- ²³P. B. Visher, Phys. Rev. B **10**, 943 (1974).
- ²⁴V. J. Emery, S. A. Kivelson, and H. Q. Lin, Phys. Rev. Lett. **64**, 475 (1990).
- ²⁵J. D. Jorgensen, B. Dabrowski, S. Pei, D. G. Hinks, L. Soderholm, B. Morosin, J. E. Schirber, E. L. Venturini, and D. S. Ginley, Phys. Rev. B **38**, 11 337 (1988).
- ²⁶V. J. Emery and S. A. Kivelson, Physica C **209**, 597 (1993).
- ²⁷G. Yu, C. H. Lee, A. J. Heeger, N. Herron, E. M. McCarron, L. Cong, G. C. Spalding, C. A. Nordman, and A. M. Goldman, Phys. Rev. B **45**, 4964 (1993).
- ²⁸H. Szymczak and R. Szymczak, A. Phys. Pol. A **85**, 79 (1994).
- ²⁹J. C. Maxwell, Nature **11**, 53 (1874).
- ³⁰W. Gibbs, Trans. Conn. Acad. Arts Sci. **3**, 108 (1988).
- ³¹V. J. Emery and G. Reiter, Phys. Rev. B **38**, 11 938 (1988).
- ³²F. C. Zhang and T. M. Rice, Phys. Rev. B **41**, 7243 (1990).
- ³³V. J. Emery and G. Reiter, Phys. Rev. B **41**, 7247 (1990).
- ³⁴H. B. Pang, T. Xiang, Z. B. Su, and L. Yu, Phys. Rev. B **41**, 7209 (1990).
- ³⁵C. D. Batista and A. A. Aligia, Phys. Rev. B **48**, 4212 (1993).
- ³⁶A. Kawabata, Prog. Theor. Phys. **48**, 1793 (1972).
- ³⁷K. Kubo, J. Phys. Soc. Jpn. **33**, 929 (1972).
- ³⁸H. Shimahara, S. Miasawa, and S. Takada, J. Phys. Soc. Jpn. **58**, 4168 (1989).
- ³⁹H. Shimahara and S. Takada, J. Phys. Soc. Jpn. **61**, 989 (1992).